The humping phenomenon during high speed gas metal arc welding

T. C. Nguyen, D. C. Weckman*, D. A. Johnson and H. W. Kerr

A commonly observed welding defect that characteristically occurs at high welding speeds is the periodic undulation of the weld bead profile, also known as humping. The occurrence of humping limits the range of usable welding speeds in most fusion welding processes and prevents further increases in productivity in a welding operation. At the present time, the physical mechanisms responsible for humping are not well understood. Thus, it is difficult to know how to suppress humping in order to achieve higher welding speeds. The objectives of this study were to identify and experimentally validate the physical mechanisms responsible for the humping phenomenon during high speed gas metal arc (GMA) welding of plain carbon steel. A LaserStrobe video imaging system was used to obtain video images of typical sequences of events during the formation of a hump. Based on these recorded video images, the strong momentum of the backward flow of molten metal in the weld pool that typically occurred during high speed welding was identified as the major factor responsible for the initiation of humping. Experiments with different process variables affecting the backward flow of molten weld metal were used to validate this hypothesis. These process variables included welding speed, welding position and shielding gas composition. The use of downhill welding positions and reactive shielding gases was found to suppress humping and to allow higher welding speeds by reducing the momentum of the backward flow of molten metal in the weld pool. This would suggest that any process variables or welding techniques that can dissipate or reduce the momentum of the backward flow of molten metal in the weld pool will facilitate higher welding speeds and productivity.

Keywords: Humping, Gas metal arc welding, GMAW

Introduction

In today's competitive manufacturing industries, there is a constant demand to improve productivity without sacrificing the overall quality of the product. For many welded products, an increase in productivity often requires use of higher welding speeds. This can be achieved through optimising or automating existing welding processes. In certain cases, switching to newer high energy density welding processes will result in higher welding speeds and increases in productivity.

With higher welding speeds, the heat input must be increased to maintain the same amount of energy input per unit length of weld required for melting of filler and base metals. Otherwise, the weld cross-section will decrease, and eventually no melting of the base metal will occur. In arc welding processes, the heat input per unit distance travelled by a moving arc can be defined by the following formula

$$\text{Heat input per unit distance} = \frac{\eta EI}{v} \quad (1)$$

where: η is the arc efficiency; E is the voltage (V); I is the welding current (A); and v is the welding speed (m s^{-1}).[1]

Theoretically, higher welding speeds can be obtained by optimising various process variables while maintaining the same heat input per unit distance, as in equation (1). This will provide the required productivity increase while retaining the same weld dimensions. However, despite having the same amount of heat input per unit distance, continued increases of the welding speed are in practice limited by the deterioration of the quality of weld bead profile. One of the most commonly occurring geometrical defects at high welding speeds is the humping phenomenon. As shown by the top view of a humped gas metal arc (GMA) weld in Fig. 1, humping can be described as a periodic undulation of the weld bead, with a typical sequence of undulation consisting of a hump and a valley. Figure 2 shows the transverse sections at a valley and a hump, respectively, of a humped GMA weld. Although the depth of penetration

Department of Mechanical Engineering, University of Waterloo, Waterloo, Ontario N2L 3G1, Canada

*Corresponding author, email dweckman@mecheng1.uwaterloo.ca

Published by Maney on behalf of the Institute
Received 19 April 2004; accepted 11 November 2004
DOI 10.1179/174329305X44134

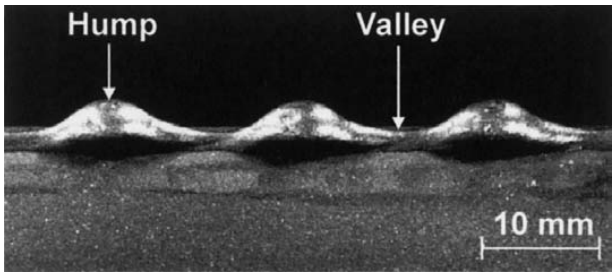

1 Bead on plate GMA weld in plain carbon steel exhibiting the humping weld defect

is the same for both transverse sections, there is more weld metal accumulation at the hump. The humping defect compromises the mechanical integrity of the weld joint, thereby limiting the welding speed and thus overall production rates. Therefore, to achieve further gains in productivity, the occurrence of humping must be suppressed or eliminated. This requires a thorough understanding of the physical mechanisms responsible for the humping phenomenon.

At higher welding speeds, the humping phenomenon has been observed in both non-autogenous welding processes, such as GMA welding,[2–4] and autogenous processes, such as gas tungsten arc (GTA) welding,[5,6] laser beam welding (LBW)[7,8] and electron beam welding (EBW).[9–11] Bradstreet[3] was the first to report the formation of humped welds during GMA welding of plain carbon steel using the spray transfer mode. He suggested that the humping phenomenon is influenced by the welding speed, the voltage, the surface condition of the workpiece, the chemical composition of the base metal, and the angle of the electrode with respect to the workpiece. He also found that reactive shielding gases such as Ar–CO_2 and Ar–O_2 mixes significantly increased the limiting welding speed before humping occurred, and argued that this was a result of the lower surface tension and improved wetting that occurred when the reactive gases were used. In later studies by Nishiguchi *et al.*,[2,4] parametric maps of arc voltage *v.* welding speed were developed for GMA welding of mild steel using short circuit metal transfer mode. These maps showed regions of process parameters that produced good weld beads and regions that resulted in humping and other weld defects. They found that humping occurred as the welding speed was increased above a certain critical welding speed and that there was an inverse relationship between this critical welding speed and the welding voltage or power used; that is, as the welding power was increased, humping occurred at lower welding speeds.

Humped welds have also been observed and studied in various autogenous welding processes. These studies include the formation of humped welds in GTA welding by Yamamoto and Shimada[5] and Savage *et al.*,[6] the formation of humped welds in LBW by Hiramoto *et al.*[7] and Albright & Chiang,[8] and the formation of humped welds in EBW by Tsukamoto *et al.*[9,10] and Tomie *et al.*[11] The humping phenomenon in these autogenous welding processes has been found to be influenced by many different welding process parameters, such as welding speed, welding power, type of shielding gas, ambient pressure, electrode geometry, travel angle and energy density at the workpiece. Several attempts have been made to express the relationship between these process

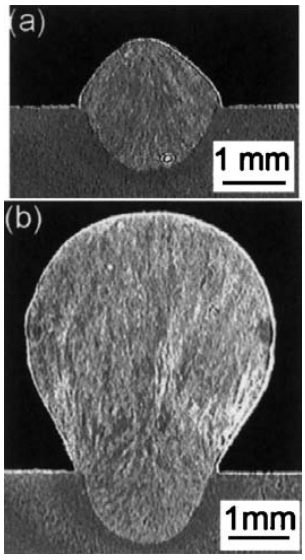

2 Transverse sections of the GMA weld shown in Fig. 1 at *a* a valley and *b* a hump

variables and the onset of humping.[3–15] The results have typically included process maps that show the onset of humping with respect to welding speed and welding current or welding power. On each of these process maps, welding process parameters such as the shielding gas composition, the ambient pressure, the torch angle or the GTA electrode geometry are normally kept constant. Any minor change to these constant process parameters will alter the results, and more experimental work is thus needed to produce new process maps.

Although the experimental results of these parametric studies clearly show the range of conditions that will result in humping when using a specific set of preset welding parameters, they do not reveal the physical mechanisms responsible for the humping phenomenon or the sequence of events taking place during the formation of a humped weld. Without direct observations, it is difficult to explain what causes the transition from good to humped welds with increased welding speed or welding power.

Despite the lack of direct observations, several models of the humping phenomenon have been proposed that are based on experimental results and observations of the final weld bead profiles. These models include the Rayleigh jet instability model by Bradstreet[3] and its modifications by Gratzke *et al.*,[15] the arc pressure model by Paton *et al.*[16] and the supercritical flow model by Yamamoto and Shimada.[5] The supercritical flow model was later adopted and modified by Mendez *et al.*[13,14] in their study of GTA welding of stainless steel. These models suggest that fluid flow, arc pressure, metallostatic pressure, capillary force and lateral instability of a cylindrical jet of molten weld metal are possible factors responsible for humping. However, the exact physical mechanism is unclear and is still being debated. Although some of the proposed models can provide plausible explanations of the periodic behaviour of the humping phenomenon, their ability to predict the onset of humping has not been experimentally demonstrated. From a practical welding perspective, these models do not provide any possible techniques or processes that allow practitioners to achieve higher welding speeds without the formation of humps.

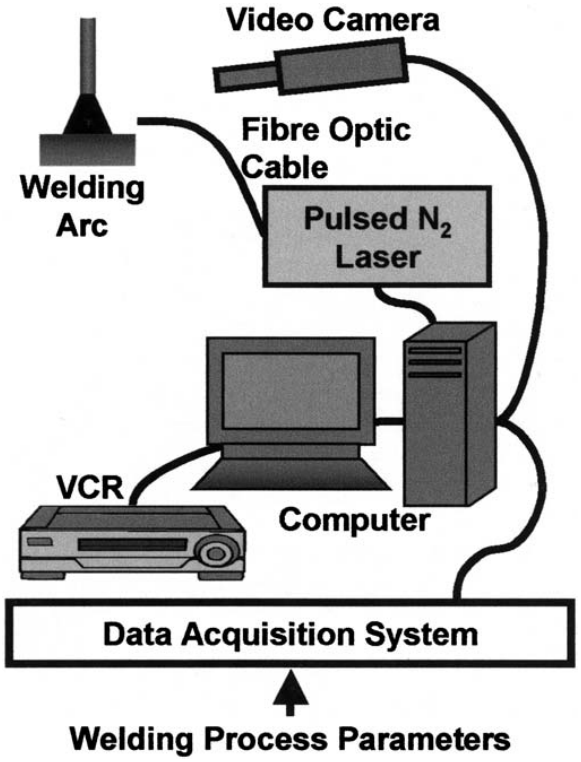

3 Various components of the LaserStrobe video imaging system

The objectives of the present study were to observe, identify and experimentally validate the physical mechanisms responsible for the humping phenomenon at high welding speeds during GMA welding of plain carbon steel. As part of the study, the effectiveness of process variables such as the type of shielding gas and welding positions on the suppression of humping were explored.

Experimental apparatus and procedure

In this study, a LaserStrobe video system[17] was used to observe and to record images of the humping phenomenon during bead on plate GMA welding of plain carbon steel plate. As shown schematically in Fig. 3, the LaserStrobe video imaging system consisted of a video camera, a video recorder (VCR), a pulsed N_2 laser strobe with fibreoptic beam delivery, a data acquisition system and a personal computer that acted as a system controller. The pulsed N_2 laser strobe was used to overwhelm the intense radiation of the GMA welding arc, since the laser light was much brighter than the light coming from the process.[17] The laser illuminated scene was viewed by a video camera equipped with a CCD video sensor, a narrow bandpass filter tuned to the 337·1 nm wavelength of the N_2 laser, and an image intensifier which was also used as a high speed electronic shutter. The computer synchronised the camera's electronic shutter with the laser pulses. The combination of temporal filtering provided by the electronic shutter, N_2 laser pulse synchronisation and spectral filtering from the narrow bandpass filter allowed unobstructed viewing of the events taking place during the formation of a humped GMA weld without the intense light from the welding arc. During filming, the video camera was mounted on a fixture that moved along with the GMA welding torch.

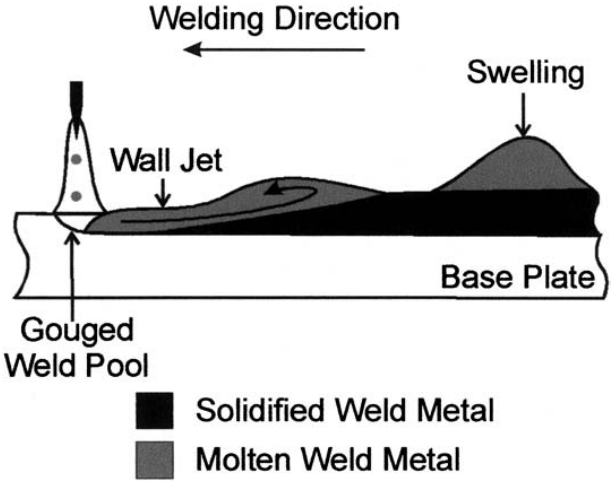

4 Definition of various terms used in the discussion of the humping phenomenon

In the present study, bead on plate GMA welds were produced on 6·5 mm thick cold rolled plain carbon steel plates using 0·9 mm diameter ER480S-6 wire and a 22 mm contact tip to workpiece distance. The welds were made using a Fanuc 6 axis welding robot and Lincoln PowerWave 455 power supply over a wide range of preset welding speeds and welding powers. To determine the usable welding speeds at each power level, the weld bead profiles were examined and the maximum welding speed that produced a non-humped weld was recorded. To observe the sequence of events taking place during humping in more detail, welds were produced using 25 mm s^{-1} welding speed, 31 V welding voltage, 20 m min^{-1} wire feed speed and argon shielding gas. These welding parameters resulted in an 8·75 kW power input. To further examine the physical mechanisms responsible for the humping phenomenon, experiments were conducted at a fixed power level using three different welding grade shielding gases, argon, Mig Mix Gold (MMG; Praxair Distribution Inc., Kitchener, ON, Canada) and TIME (BOC Gases Canada Ltd, Waterloo, ON, Canada), and three welding positions (10° uphill, flat and 10° downhill). The composition of each shielding gas is listed in Table 1. In this study, argon was an inert shielding gas, while MMG and TIME were reactive shielding gases, due to their O_2 and CO_2 contents. In the design of experiments, the wire feed speed was set at 15 m min^{-1} and the voltage was set at 29 V, 31·5 V and 32·5 V for argon, MMG and TIME shielding gases, respectively. These process parameters produced 7·5 kW welding power and spray transfer condition for all welds.

Results and discussion

The humping phenomenon

To facilitate discussion of the humping phenomenon, a schematic diagram in Fig. 4 is used to illustrate the definition of various terms. This diagram shows the

Table 1 Composition of shielding gases

Shielding gas	Composition
Argon	100% Ar (Ultra High Purity Grade)
Mig Mix Gold™	92% Ar, 8% CO_2
TIME™	65% Ar, 8% CO_2, 26·5% He, 0·5% O_2

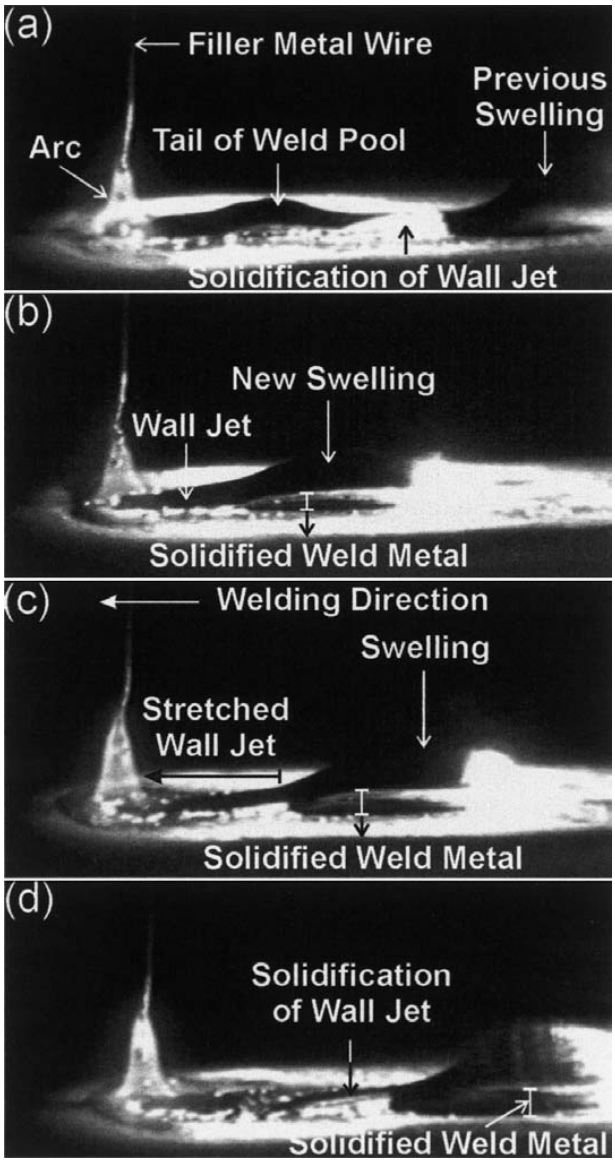

5 LaserStrobe video images showing a typical sequence of events during the formation of a humped bead on plate GMA weld

longitudinal section along the centreline of a humped GMA weld. The term 'swelling' is used to describe the accumulation of molten weld metal that occurs during welding. Upon solidification, these swellings become the humps observed in a defective weld (Fig. 1). According to the work of Bradstreet[3] and Mendez *et al.*,[13,14] high arc pressure and the momentum of the molten filler metal droplets depress the surface of the weld pool directly under the arc, creating a gouged weld pool. The molten filler and base metals flow in two channels that surround the welding arc as well as within a very thin layer located underneath the welding arc.[13,14] Immediately behind the welding arc, these separated flows merge to form a combined stream of molten weld metal. As shown in Fig. 4, this combined stream of molten weld metal continues to flow towards the tail of the weld pool. In this study, the term 'wall jet'[18] is used to describe this combined stream of molten weld metal that runs along the fusion boundary from the welding arc towards the tail of the weld pool as illustrated in Fig. 4.

As the first step in the quest to understand the humping phenomenon, the sequence of events taking place during the formation of a humped weld was filmed using the LaserStrobe video imaging system. In Fig. 5, four LaserStrobe video images chronicle the sequence of events that were typically observed during the formation of a humped GMA weld. Since the humping phenomenon is periodic in nature, the first frame, Fig. 5*a*, begins at the completion of a previous hump. The filler metal wire, the welding arc and the new tail of the weld pool are labelled in this frame. Within the welding arc, filler metal droplets are clearly visible. In these LaserStrobe video images, it was possible to distinguish between molten and solidified weld metal. There was more diffuse reflection of the N_2 laser light directly from the solidified weld metal surface back into the video camera, resulting in the bright fields observed in Fig. 5*a*. On the other hand, there was mostly specular reflection off the clean molten metal surface, and this was seldom reflected back towards the camera, due to the relative orientation of the molten metal surface to the video camera. Thus, molten weld metal was typically black in these images.

As shown in Fig. 5*a*, a portion of the weld, connecting the previous swelling and the new tail of the weld pool, had completely solidified, although the upper region of the previous swelling was still molten. Prior to solidification, this portion of the weld was part of the wall jet that supplied the swelling with molten weld metal. The solidification of the wall jet is an important event, since it signals the completion of one hump and subsequently the beginning of another.

During the humping phenomenon, the molten filler and base metals were displaced from the front towards the tail of the weld pool within the wall jet. In Fig. 5*b*, at the tail of the weld pool, the molten weld metal accumulated to form a new swelling. In fact, the humps were periodic accumulations or swellings of molten weld metal that first formed and then solidified during high speed welding. Although its size was increasing, the new swelling was stationary with respect to the baseplate. This prevented the recirculation of molten weld metal towards the front of the weld pool as described by Bradstreet.[3] As a consequence, backfilling of the front portion of the weld pool did not occur. Meanwhile, the welding arc continued to move to the left along the weld joint at the preset welding speed. As illustrated by Fig. 5*b* and *c*, the wall jet became elongated over an ever increasing distance between the forward moving welding arc and the stationary swelling. Also, the thermal mass of molten metal inside the wall jet had been distributed over a longer distance, making it vulnerable to rapid solidification, which would choke off the flow of molten metal to the swelling.

While the molten metal was accumulating in the swelling, solidification of the molten weld metal in the swelling and the wall jet occurred (Fig. 5*b* and *c*). As indicated in the images of Fig. 5*b* and *c*, the bright region of solidified metal increased in height as the solidification of the molten weld metal proceeded upwards. The wall jet solidified completely once the height of solidified weld metal was approximately equal to that of the wall jet (Fig. 5*d*). Solidification of the wall jet formed the valley typically observed between swellings in a humped GMA weld bead (as shown in Fig. 1)

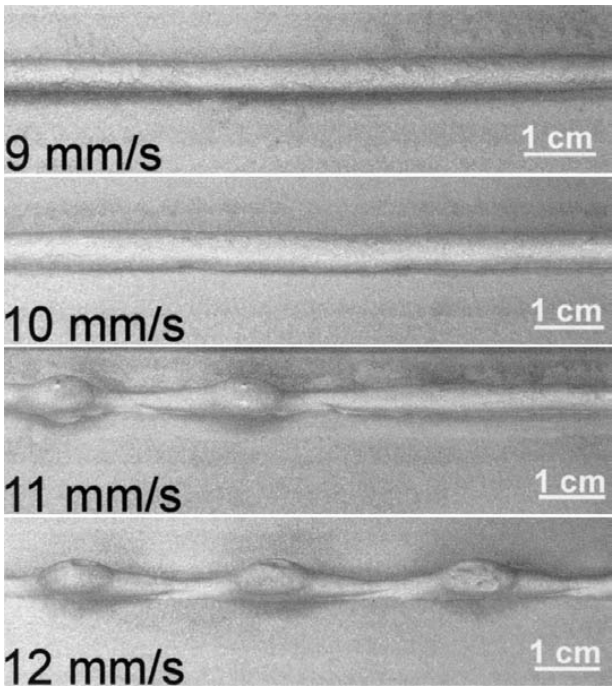

6 Top view of GMA welds produced using 6·3 kW welding power and argon shielding gas, at various welding speeds

and choked off the flow of molten weld metal to the swelling. This was soon followed by the initiation and growth of a new swelling closer to the arc and further along the weld bead (Fig. 5*a*).

The images in Fig. 5 illustrate the typical sequence of events that take place during the formation of a humped GMA weld such as that shown in Fig 1. The accumulation or the swelling of molten weld metal and solidification of the wall jet signal, respectively, the start and the end of a humping sequence. Initially, a new swelling was formed because the flow passage of the molten weld metal to the previous swelling had been blocked by the solidification of the wall jet. Despite the fact that the arc was moving forwards at high welding speed, the swelling continued to grow in size by receiving more molten weld metal from the front of the weld pool via the new wall jet. Based on this observation, the fluid flow within the wall jet must be predominantly towards the tail of the weld pool, with high velocity and momentum. This high velocity, rearward directed flow of molten weld metal in the weld pool is consistent with numerical simulations by Beck *et al.*[19] and observations in tandem EBW by Arata and Nabegata.[20]

As indicated by the height of the swelling in Fig. 5, the molten weld metal must have a high surface tension to contain a large amount of metal within the swelling. As demonstrated in the latter part of this article, when the surface tension is low, the molten weld metal will overflow the sides of the weld pool and flatten out onto the surface of the baseplate. As a result, no swelling or hump will form. Since the swelling is constrained by its high surface tension, yet continued to further increase in size, the backward flow of molten weld metal must have high velocity and momentum. Thus, the momentum of the backward flow of molten weld metal is responsible not only for the initial formation but also for the growth of the swelling.

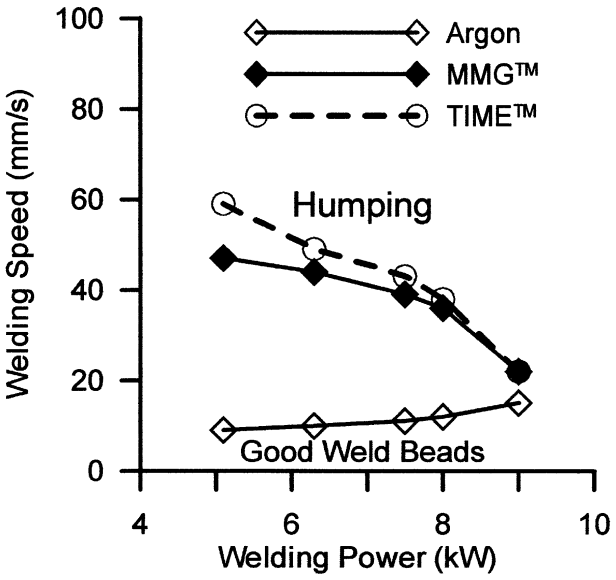

7 Plot of limiting welding speeds *v.* welding powers for argon, MMG and TIME shielding gas

As shown in Fig. 5, the swelling increases its size by bulging upwards and is stationary with respect to the baseplate. Since the swelling is stationary and there is a strong backward flow of molten weld metal in the wall jet, the forward recirculation of molten metal described by Bradstreet[3] does not occur. As a result, backfilling of the front portion of the weld pool is not possible. The lack of backfilling causes the elongation and ultimately the solidification of the wall jet to form a valley in the humped weld bead (Fig. 1). This solidification and choking off of the flow in the wall jet will lead to the formation of a new accumulation or a new swelling further down along the weld joint and closer to the arc. Thus, the high velocity and momentum of the backward directed flow of molten metal in the weld pool prevents backfilling of the front portion of the weld pool.

Figure 6 shows the top view of GMA welds produced using 6·3 kW welding power, argon shielding gas and 9, 10, 11 and 12 mm s^{-1} welding speeds, respectively. In Fig. 6, the welds produced at 9 mm s^{-1} and 10 mm s^{-1} welding speeds were classified as good welds, since the weld beads show no significant variation in weld dimensions or shape along the length of the weld. However, at 11 mm s^{-1} welding speed, the weld bead begins to exhibit intermittent swellings that are separated by valleys. The occurrence of the humps and valleys becomes consistently periodic at 12 mm s^{-1} welding speed. Thus, the difference between good weld beads and a humped weld can be clearly identified by the significant variations in weld bead dimensions and shape that occur along the length of the humped weld bead and the periodic occurrence of humps and valleys. Based on the weld beads shown in Fig. 6, the limiting welding speed for production of good argon shielded GMA welds using 6·3 kW welding power was 10 mm s^{-1}.

Figure 7 shows the relationship between the limiting welding speeds as defined above by the appearance of humping and the welding power for GMA welds produced using argon, MMG and TIME shielding gases. In this graph, the lines represent the limiting welding speed. The region below each line represents various welding speed and power combinations that

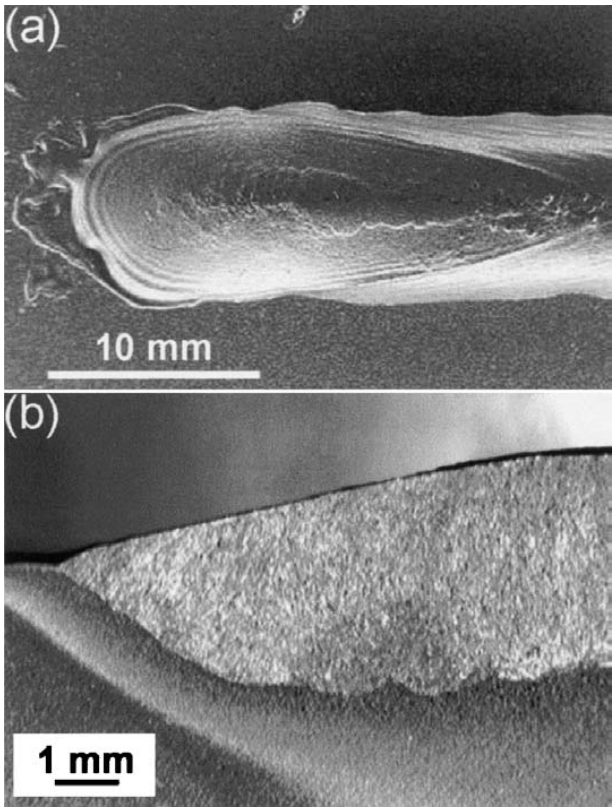

a Top view; *b* Longitudinal section

8 GMA weld produced using 8 kW welding power and argon shielding gas, at 10 mm s^{-1} welding speed

produced good weld bead profiles. On the other hand, above each line is a region of conditions that produced humped welds.

From the experimental results shown in Fig. 7, at lower power levels the use of TIME shielding gas resulted in higher limiting welding speeds than was possible when using MMG shielding gas. However, this advantage of the TIME shielding gas diminished with increased welding power. At 6·0 kW power input, the limiting welding speed when argon was used was found to be about 10 mm s^{-1}, whereas welding speeds up to 44 mm s^{-1} were possible with the reactive MMG shielding gas, and speeds up to 60 mm s^{-1} were possible with the TIME gas. This represents an increase in productivity of between 440% and 600% relative to that possible with pure argon shielding gas at this welding power. When MMG and TIME shielding gases were used, the limiting welding speed decreased as the welding power increased. This trend is very similar to those reported in previous studies of the humping phenomenon.[2,5–12] The same trend, however, does not exist for welds produced using argon shielding gas. In this case, higher welding speeds were possible with higher welding powers. Consequently, the increase in welding speed and productivity with reactive shielding gases was less pronounced at higher welding powers (e.g. 9 kW).

As plotted in Fig. 7, for the same reactive shielding gas, the limiting welding speed above which humping occurred was observed to decrease with increased power; that is, humping would occur with increased welding speed at the same power level or increased power at the same welding speed. As discussed previously, the momentum of the backward flow of molten weld metal

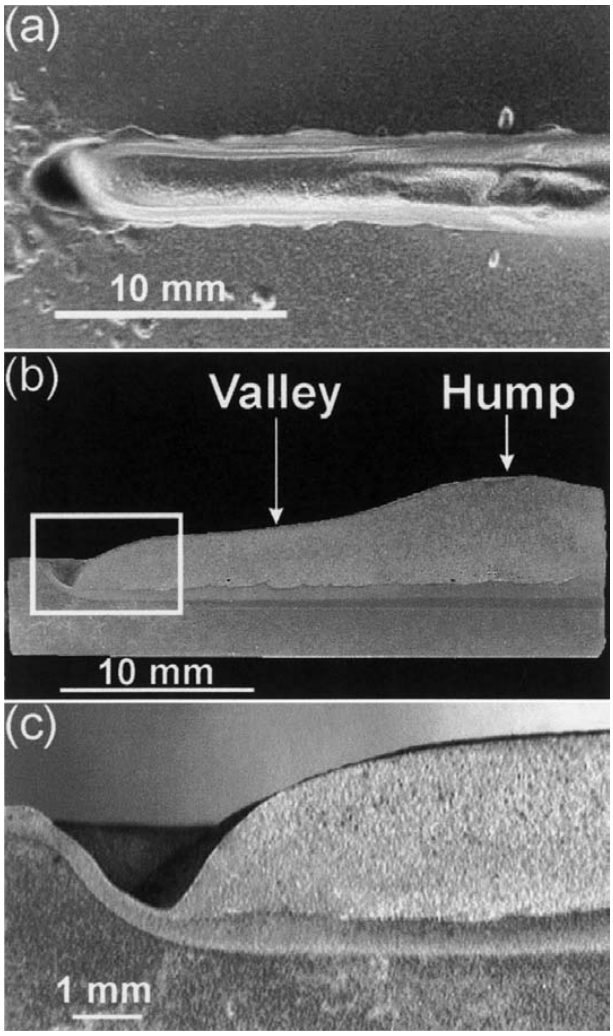

a Top view; *b* Longitudinal section; *c* Close-up view of the gouged weld pool

9 GMA weld produced with 8 kW welding power and argon shielding gas, at 20 mm s^{-1} welding speed

is responsible for the initial formation and growth of the hump as well as the formation of the valley. When either the power or the welding speed is increased, it can be assumed that the velocity and momentum of the flow of molten metal towards the tail of the weld pool must also be higher. To properly understand the humping phenomenon, it is essential to identify and to understand the physical mechanisms that are responsible for the increased momentum of the backward flow of molten weld metal.

Figures 8 and 9 show the top and the longitudinal views of weld craters produced using the same welding parameters, but at 10 mm s^{-1} and 20 mm s^{-1} welding speeds, respectively. A good weld bead was produced at 10 mm s^{-1}, while a humped weld bead was observed at 20 mm s^{-1}. At 10 mm s^{-1} welding speed, the weld is wider and deeper than the weld produced at 20 mm s^{-1}. At a welding speed of 10 mm s^{-1}, there is no visible depression of the weld pool surface (Fig. 8). During welding, the weld pool surface might have been slightly depressed by the arc forces and the impingement of the filler metal droplets. However, any depression of the free surface was backfilled by the recirculation of molten weld metal towards the front of the weld pool after the welding arc was turned off. As a result, the final weld

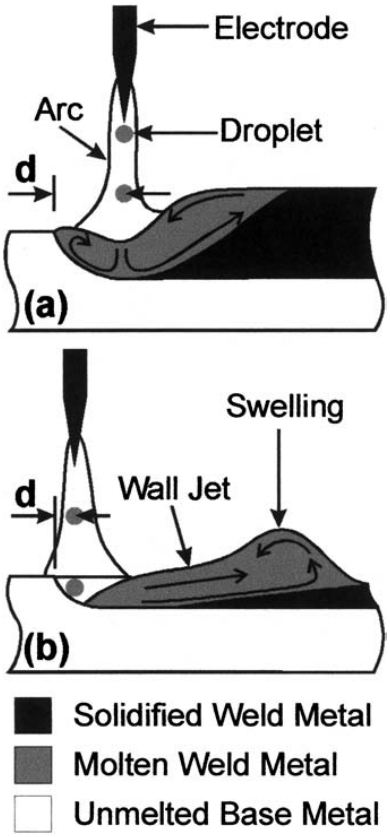

a Low welding speed; *b* High welding speed

10 Longitudinal sections of the weld pool and the filler metal droplet impingement locations

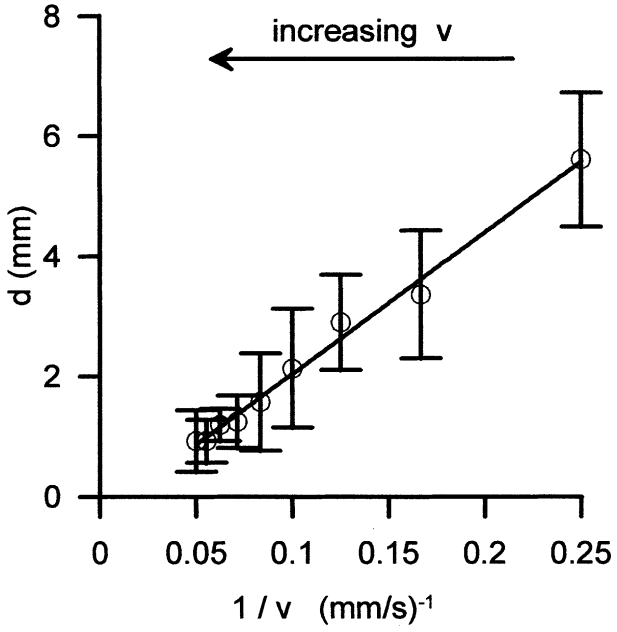

11 The measured distance between the weld pool leading edge and the molten filler metal entrance location *d* as a function of the inverse of welding speed *v*

profile does not show any sign of surface depression. Meanwhile, at 20 mm s^{-1} welding speed, the weld pool was heavily gouged (Fig. 9) by the combined actions of the high arc forces and the molten metal droplets impinging on the inclined surface of the leading edge of the fusion boundary. Since this gouged weld pool retained its shape after the welding arc had been turned off, there was no time for recirculation of the molten weld metal towards the front of the weld pool prior to solidification of all molten metal.

Figure 10 shows schematic diagrams of longitudinal sections of welds produced using the same set of welding parameters, but at low and high welding speeds. On these diagrams, *d* is the longitudinal distance along the weld centreline from the leading edge of the weld pool to the location where the filler metal droplet impinges on the top surface of the weld pool. As illustrated in Fig. 10*a*, during low speed welding, the molten weld metal is normally contained within a large weld pool underneath the welding arc. The depression of the free surface of the weld pool due to arc force and the filler droplet momentum is possible, but limited by the forward recirculation of the molten weld metal.[16] This relatively large pool of molten metal can be expected to absorb and dissipate the momentum of the incoming filler metal droplets in the GMA welding process. Consequently, the backward momentum of molten metal within this weld pool is low and there is little chance of forming a humped weld.

As illustrated in Fig. 10*b*, at high welding speed, the weld pool becomes elongated, shallow and narrow. Meanwhile, the electrode, the welding arc and the metal droplet stream move forwards and closer to the leading edge of the weld pool. Owing to the reduction in penetration and volume or mass of molten metal in the weld pool, the combined actions of the arc forces and the droplet momentum create a depression or gouged region at the front of the weld pool that contains a very thin layer of liquid metal underneath the welding arc. Without the presence of a thick liquid layer underneath the welding arc, the momentum of the incoming filler metal droplets will not be absorbed or dissipated. Rather, the droplets will hit the sloping leading edge of the weld pool, as is shown schematically in Fig. 10*b*. The molten filler metal will then be redirected towards the tail of the weld pool at high velocity, dragging with it any liquid metal in the front of the weld pool. Backfilling of the front portion of the weld pool does not occur, because the recirculated molten weld metal fails to keep up with the forward moving welding arc and is pushed or held back by the high velocity fluid flow within the wall jet.

The plot of Fig. 11 shows the longitudinal distance measured from the weld pool leading edge to the filler metal droplet impingement locations *d v.* the inverse of the welding speed (i.e. 1/*v*). The distance *d* is as previously defined in Fig. 10. These distances were directly measured from at least 10 LaserStrobe video images of GMA welds produced using 7·5 kW, flat welding position, argon shielding gas and a range of welding speeds. The error bars represent ± 3 standard deviations of the measured data. As shown in Fig. 11, the distance *d* decreases with increased welding speeds. In addition, there is less scatter in the measured data with increased welding speeds. The experimental results of Fig. 11 indicate that the impingement location of filler metal droplets is more concentrated and moves closer to the leading edge of the weld pool as the welding speed is increased. As shown in Fig. 9, at high welding speeds, the front of the weld pool is often gouged out. As the filler metal droplets impinge on the

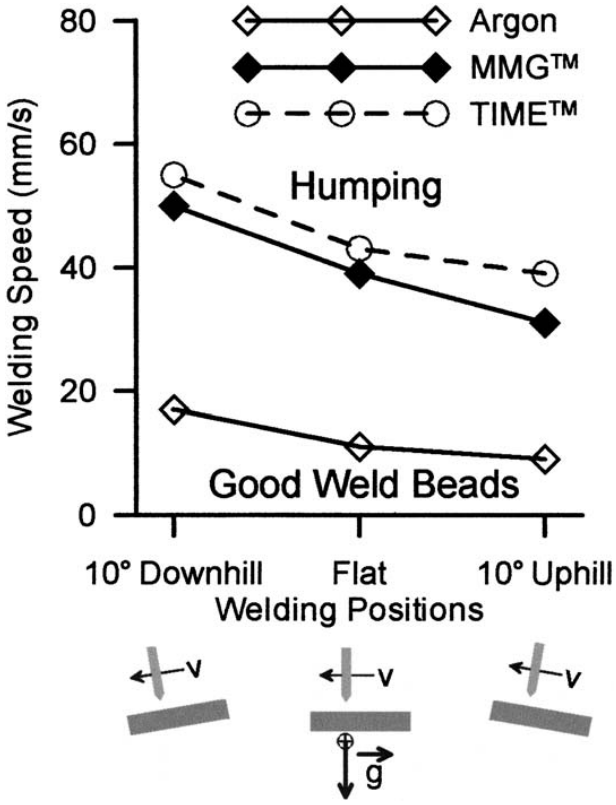

12 The influence of welding positions on limiting welding speeds for welds made using 7·5 kW welding power and different shielding gases

sloping leading edge of a gouged weld pool, the exposed base metal at the leading edge behaves like a deflecting vane. The momentum of the incoming filler metal droplets will be redirected towards the back of the weld pool. As a result, there is an increase in the momentum of the backward flow of molten metal, which will promote the formation of a humped weld. This explains the occurrence of humping at higher welding speeds for the same power input.

As shown in Fig. 7, humping occurs with increased power at the same welding speed. To increase the power in GMA welding, both the wire feed speed (and consequently the welding current) and the preset welding voltage must be increased. High welding currents have several effects that promote the early onset of humping. First, high welding current causes an increase of the arc force that depresses the weld pool surface, thus creating a gouged region that is typically observed directly underneath the welding arc.[21,22] As previously explained, the sloping leading edge of a gouged weld pool redirects the incoming filler metal droplets towards the tail of the weld pool at high velocity. Second, the viscous drag force of the plasma gas, which influences the momentum of the molten weld metal within the weld pool, is much stronger at higher welding currents.[13,14] This viscous drag force of the plasma gas further increases the flow velocity and momentum of molten weld metal towards the tail of the weld pool. Both the rearward deflecting action of the leading edge of a gouged weld pool and the high viscous drag force of the plasma gas increase the overall velocity and momentum of the backward flow of molten weld metal. As a result, at the same welding speed, humping will occur as the welding power is increased.

Suppressing the onset of humping

If the strong backward flow of the molten weld metal is responsible for the formation of humped weld, then any process variables or welding techniques that reduce the momentum of this flow will allow higher welding speeds without the humping defect. To validate this hypothesis, experiments were conducted using gravitational force and shielding gases as means to influence the momentum of the backward flow of molten metal in the weld pool. In addition, the different shielding gases were also used to influence the surface tension of the molten weld metal.

Figure 12 shows the limiting welding speeds at three different welding positions for welds produced using 7·5 kW welding power and argon, MMG and TIME shielding gases, respectively. In addition, schematic diagrams are included in this figure to illustrate the various welding positions with respect to the gravitational force g. In Fig. 12, each curve represents the limiting welding speed. Below the curve is a region in which good weld beads were produced. Conversely, humping was observed when the welding speed exceeded the limiting welding speed curve. From the experimental results, the limiting welding speeds are influenced by both the welding positions and the types of shielding gas. Similar to the results shown in Fig. 7, the limiting welding speeds of the reactive shielding gases were approximately 300% greater than that possible when using pure argon shielding gas. In Fig. 12, at 7·5 kW welding power, there was a smaller, but consistent, increase in the limiting welding speed obtained when using the TIME shielding gas relative to the MMG shielding gas.

In Fig. 12, use of the 10° downhill position allowed higher limiting welding speeds than the flat position. In turn, higher limiting welding speeds were possible in the flat welding position than in the 10° uphill welding position. With downhill welding, the molten weld metal must flow uphill and against the gravitational force while being displaced towards the tail of the weld pool. Once the momentum of the backward flow of molten weld metal has been weakened by the influence of gravity, it is difficult to form an accumulation of molten metal at the tail of the weld pool, and backfilling of the front portion of the weld pool occurs more readily. As a consequence, higher limiting welding speeds were realised with the 10° downhill welding position. Conversely, during uphill welding, the momentum of the backward flow of molten weld metal was increased by the gravitational force, thereby promoting humping at lower welding speeds. As a result, with 10° uphill welding position, the limiting welding speeds were the lowest. By changing the welding position with respect to the gravitation force orientation, the momentum of the backward flow of molten weld metal has been altered, which results in different limiting welding speeds. These results demonstrate that the momentum of the backward flow of molten weld metal is a major factor responsible for the humping phenomenon and that the orientation of the gravity force can be used effectively to suppress humping; that is, higher welding speeds are made possible by welding downhill. In practice, this can be easily accomplished by clamping the weldment in a slightly inclined orientation and welding downhill. This concept may be extended from the making of simple

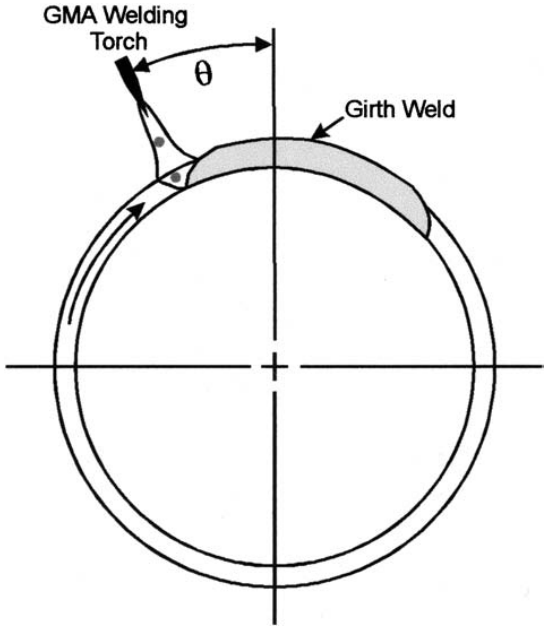

13 High speed GMA girth welding where the torch is fixed at an angle θ and the the two pipes or cylinders are rotated during welding

linear welds to the making of cylindrical girth welds, where the welding torch is fixed and the two pipes or cylinders are rotated during welding, as shown in Fig. 13. In this case, higher welding speeds should be possible when the welding torch is moved forwards by an optimised angle, θ, such that the weld is effectively being made in the downhill position relative to the gravity vector, $\vec{g}$.

From the experimental results shown in Fig. 12, it can be seen that switching from an inert shielding gas such as argon to more reactive shielding gases such as MMG and TIME enabled higher limiting welding speeds to be obtained. It is therefore essential to understand the effects of shielding gas on the formation of humps in GMA welds. Figure 14 shows transverse sections of GMA welds produced using argon, MMG and TIME shielding gases. These welds were produced using 7·5 kW welding power and 11 mm s^{-1} welding speed, and were made in the flat welding position. On each photomicrograph, θ_c is the acute contact angle between the baseplate surface and the top surface of the weld reinforcement.

As shown in Fig. 14, the welds produced using MMG and TIME shielding gases have flatter and wider weld beads than the weld produced using argon. In Fig. 14*a*, when the weld was made using argon shielding gas, the contact angle between the weld metal and the original surface of the workpiece was approximately 90° (π/2 radians). This large contact angle indicates a lack of wetting between the molten weld metal and the baseplate surface. It is a direct result of the high surface tension of the molten weld metal.[23] When the reactive shielding gases were used, the contact angle was much smaller and hence the surface tension of the molten weld metal must be lower. In these latter cases, the molten weld metal reacted with the O_2 in the reactive shielding gases to lower its overall surface tension. These observations are consistent with experimental measurements of the surface tension of molten steel droplets by

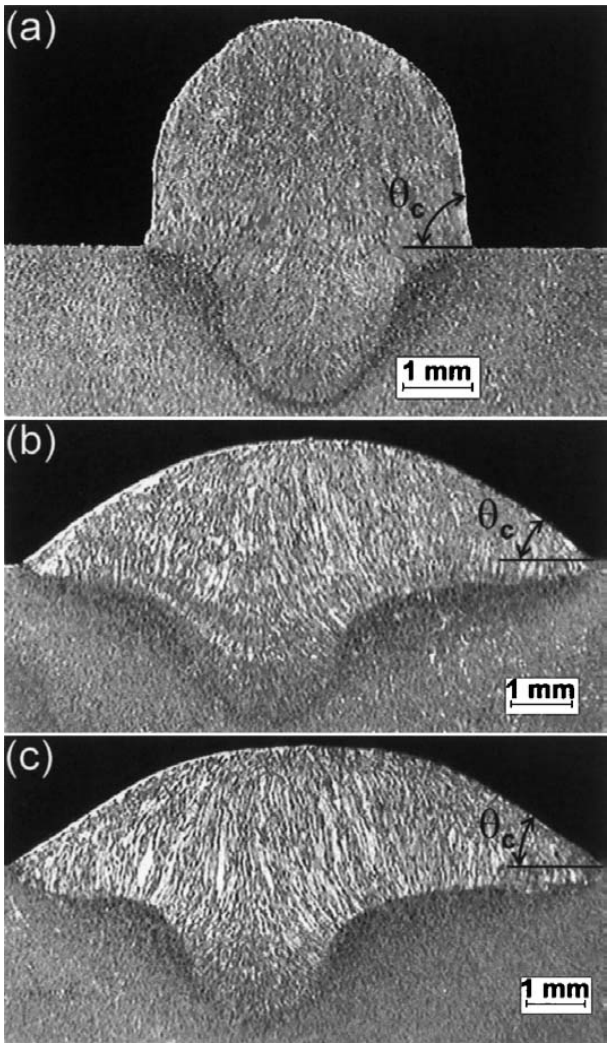

14 Transverse sections of bead on plate GMA welds produced using 7·5 kW welding power and 11 mm s^{-1} welding speed in the flat position with *a* argon, *b* MMG and *c* TIME shielding gases. θ_c is the contact angle

Subramaniam and White.[24] As previously mentioned, for a humped weld, the liquid metal must have a high surface tension to allow the swelling to accumulate a large amount of molten metal. Otherwise, the molten weld metal would flatten out over the surface of the baseplate, as seen in Fig. 14*b* and *c*, making it more difficult for a swelling to form.

In their analogous study of bead geometry stability, Schiaffino and Sonin[25] projected a fine stream of microcrystalline wax droplets onto the surface of a moving plate of Plexiglass and found that the contact angle between the molten wax and the surface of the Plexiglass workpiece was responsible for the instability of the wax bead geometry. When this angle was less than 90° (π/2 radians), humping would not occur. With a switch to reactive shielding gases, the humping phenomenon was temporarily suppressed and the contact angle between molten wax and the baseplate surface was observed to be less than 90° (π/2 radians). Their proposed bead instability model appears to be consistent with observations made in the present study of weld bead instability and humping during GMA welding. However, as shown in Figs 7 and 12, humping did eventually occur at much higher welding speeds despite

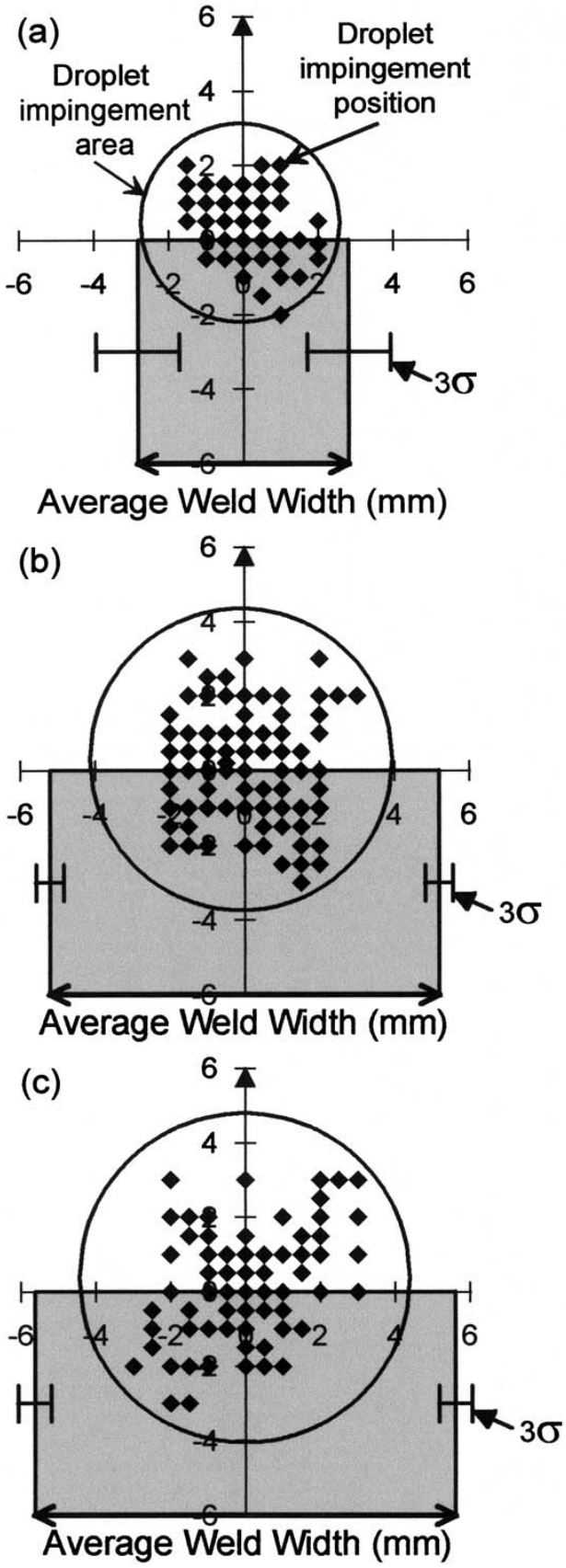

15 The filler metal droplet impingement positions and areas and the average width of welds produced using 7·5 kW welding power and 11 mm s^{-1} welding speed in the flat position when using *a* argon, *b* MMG and *c* TIME shielding gases

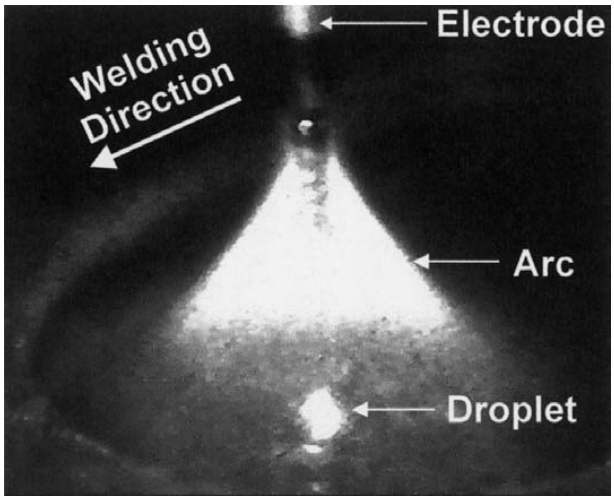

16 An example of a LaserStrobe video image showing the filler metal droplet impingement location at the weld pool top surface

the low contact angle between molten weld metal and the workpiece obtained when the reactive shielding gases were used (Fig. 14). This would suggest that the critical contact angle criterion proposed by Schiaffino and Sonin[25] is not sufficient for predicting the onset of humping in GMA welding.

One additional benefit of having a wider weld is the increase in opposing viscous drag force from the fusion boundary. From Fig. 14, it can be seen that GMA welds produced using MMG and TIME shielding gases have wider liquid/solid interfaces than the welds produced using argon shielding gas. The wider liquid/solid interface provides more viscous drag forces from the stationary fusion boundary over which the molten weld metal flows. This additional viscous drag will further oppose the backward flow of the molten weld metal. As a result, the momentum of the backward flow of molten weld metal will be reduced, thereby decreasing the likelihood of a humped weld being formed. In general, switching from an inert to more reactive shielding gases suppresses the humping phenomenon until higher welding speeds are obtained, due to the effect of the reactive shielding gases on the surface tension and resultant contact angles of the molten weld metal relative to the plate.

Besides its influence on the surface tension of the molten weld metal, the shielding gas also affects the way in which filler metal droplets impinge on the top surface of the weld pool. The average weld widths and their three standard sample deviations σ are plotted in Fig. 15. The welds were produced using 7·5 kW welding power, 11 mm s^{-1} welding speed and three different shielding gases. The grey area schematically represents the average width weld. In each plot of Fig. 15, the filler metal droplet impingement locations on the top surface of the weld pool are also plotted as data points. Impingement locations were obtained from a series of LaserStrobe video images recorded during welding. Figure 16, for example, shows a LaserStrobe video image of a droplet impinging on the weld pool top surface. The x–y coordinate of the impingement location was determined with respect to the centre of the GMA welding gun by manually superimposing a properly scaled grid onto the image. For each experimental data set, the centroid of the impingement locations, the average radius from the centroid and the

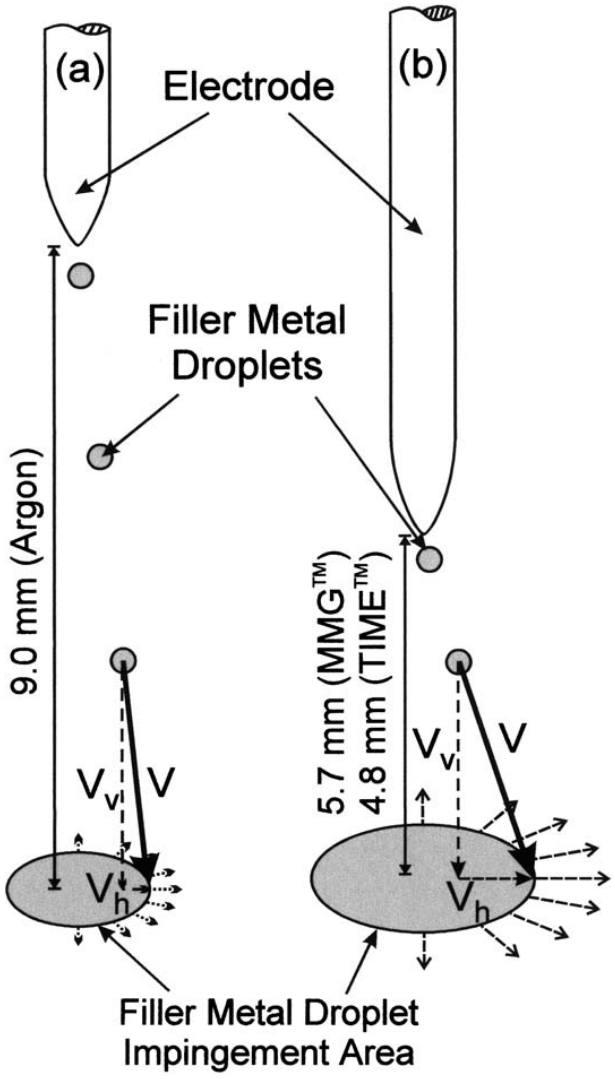

17 Difference in the overall velocity *V*, as well as the difference in horizontal and vertical velocity components V_h and V_v, of the filler metal droplets when using *a* argon and *b* MMG or TIME shielding gases

sample standard deviation of the radius were determined. The average radius from the centroid plus 3 standard deviations was plotted as a circle to symbolise the droplet impingement area in each plot of Fig. 15. Statistically, 99% of the filler metal droplets should enter the weld pool inside the area circumscribed by the circle.

Overall, the weld width and the area over which the filler metal droplets impinged on the weld pool when argon shielding gas was used were smaller than those of the welds produced with MMG or TIME shielding gases (Fig. 15). Also, there was more variation in the width of the weld produced with argon than in those of welds produced with either MMG or TIME gases. For the weld produced with argon shielding gas, the average weld width was only slightly larger than the diameter of the area over which the filler metal droplets impinged on the weld pool. On the other hand, the average weld width of the welds produced with the reactive gases was much larger than the diameter of the droplet impingement area. This observed difference is probably caused by the fluid flow pattern within the weld pool, which also has a direct impact on the formation of humps.

With use of the aforementioned welding parameters, the average arc length for the weld produced using argon shielding gas was 9·0 mm. As illustrated in Fig. 17*a*, the longer and more concentrated arc will create higher vertical arc forces,[21,22] which will depress the surface of the weld pool, creating a gouged region. With a small droplet impingement area, the magnitude of the horizontal velocity component of the filler metal droplets is small, while the magnitude of the vertical velocity component is large. The incoming filler metal droplets with high vertical velocity components will depress the weld pool surface. In addition, there is a greater distance over which the droplets will be accelerated to higher velocities by the plasma gas. At higher welding speeds, the weld penetration and width will decrease. With high vertical velocity components, the filler metal droplets depress or displace enough molten metal directly underneath the arc to create a gouged weld pool. In a gouged weld pool, the sloping leading edge redirects subsequent filler metal droplets towards the tail of the weld pool at high velocity. This increases the overall momentum of the backward flow of molten weld metal and consequently increases the likelihood of forming a humped weld. Therefore, for welds produced with argon shielding gas, humping occurs at lower limiting welding speeds (Figs 7 and 12).

As mentioned previously, the vertical velocity component of the incoming droplets will be redirected by the sloping leading edge of a gouged GMA weld pool towards the tail of the weld pool at high velocity. Meanwhile, the horizontal velocity component of the incoming droplets will determine whether the molten metal will flow laterally towards the two sides of the weld pool. With the incoming filler metal droplets having a small horizontal velocity component, the fluid flow within an argon shielded weld pool is predominantly backward with a very small amount of lateral movement. Therefore, the final weld width is of similar dimension as the diameter of the impingement area.

As shown in Fig. 17*b*, the average arc lengths of the welds produced with reactive shielding gases were 5·7 mm and 4·8 mm for MMG and TIME gases, respectively. Both of these arc lengths are much shorter than the 9·0 mm arc length of the argon shielded weld. As illustrated in Fig. 17*b*, the short arc length and large droplet impingement area reduce the magnitude of the vertical velocity component of the metal droplets, but increase the magnitude of the horizontal velocity component of the incoming filler metal droplets. As previously discussed, with smaller vertical velocity components, the incoming filler metal droplets would not be expected to greatly depress the weld pool surface or gouge the weld pool. Without a gouged weld pool, the rearward deflecting action of incoming filler metal droplets by the weld pool lead edge would not occur. As a result, the backward flow and momentum of the molten weld metal would be reduced. In addition, the large horizontal velocity component allows the molten metal to flow laterally towards the sides of the weld, carrying with it thermal energy to increase the weld width. Along with the flattening effect due to the low surface tension, the weld width produced using reactive gases is much larger than the diameter of the filler metal droplet impingement area (Fig. 15*b* and *c*). Owing to the

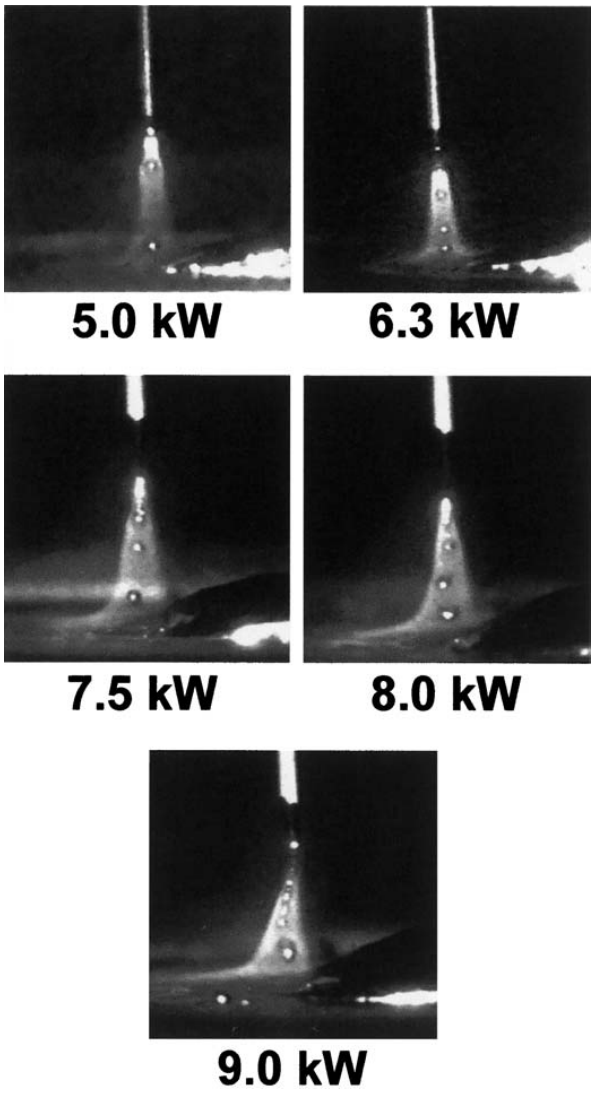

18 The effect of welding power on the flight path of filler metal droplets for welds produced using argon shielding gas

reduction in the momentum of the backward flow of molten weld metal, humping is suppressed until higher welding speeds are obtained.

In Fig. 7, the limiting welding speed for welds produced using reactive shielding gases decreased with increasing welding power. However, for welds produced using argon shielding gas, there is a slight increase in limiting welding speed with higher welding powers. This contradicts the results with reactive shielding gases as well as the results from previously published studies of the humping phenomenon.[2,5–12] As previously explained, the momentum of the backward flow of molten weld metal will increase at higher welding powers, due to the viscous drag force of the plasma gas and the rearward deflecting action of the leading edge of the gouged weld pool. The momentum increase will cause humping to occur at lower welding speeds as the welding power is increased. However, for argon shielded welds, something else has happened to allow higher limiting welding speeds at higher welding powers.

Figure 18 contains five LaserStrobe video images showing the filler metal droplets as they are being transferred across the welding arc at 5·0 kW, 6·3 kW, 7·5 kW, 8 kW and 9 kW, respectively. The welds were made using argon shielding gas and 10 mm s^{-1} welding speed. When the welding power is less than 7·5 kW, the mode of metal transfer is streaming spray transfer. The flight path of the filler metal droplets coincides with the axis of the consumable electrode. At and beyond 7·5 kW of welding power, the streaming spray transfer became a 'swinging' spray transfer mode.[26] As shown in Fig. 18, in this transfer mode, the filler metal droplets are swung around the weld pool while being detached from the end of the electrode. The swinging action reduces the vertical velocity component of the filler metal droplets, lessens the impact force that can depress or gouge the weld pool and enlarges the impingement area on the weld pool surface. In addition, the swinging flight path of the filler metal droplets prevents all of them from hitting the leading edge of the gouged weld pool. These combined effects reduce the momentum of the backward flow, which temporarily suppresses the humping phenomenon until higher welding speeds are obtained. As a result, there is a small increase in welding speed limit at higher welding powers due to the transition from streaming to swinging spray transfer that takes place with increasing welding powers.

Summary

From observations of LaserStrobe video images taken during the formation of humped GMA welds made in plain carbon steel, the backward flow of molten weld metal in the weld pool is responsible for the initial formation and the growth of a hump. In addition, the formation and the growth of a hump are promoted by the high surface tension of molten weld metal. The strong momentum of the backward flow of molten metal inside the wall jet prevents backfilling of the front portion of the weld pool. This leads to the elongation and ultimately the solidification of the wall jet to form a valley in a humped weld bead.

The deflection of the filler metal droplets by the sloping leading edge of a gouged weld pool and the viscous drag force from the plasma gas contribute to the strong backward flow of molten weld metal. Both the gouged weld pool and the strong viscous drag force from the plasma gas are the result of high welding speed and welding power.

Experiments with different welding positions and shielding gases were performed to explore the effects that the backward flow of molten weld metal has on humping. With a 10° downhill welding position, the gravitational force weakens the backward flow of molten weld metal and allowed higher welding speeds without the formation of humping. Conversely, a 10° uphill welding position strengthens the backward flow of molten metal within the weld pool and causes humping to occur at lower welding speeds. Therefore, higher welding speeds and improved productivity are possible by orienting the weldment such that welding is done in the downhill position.

Use of reactive MMG and TIME shielding gases suppresses the occurrence of humping and allows up to 400% higher welding speeds than are possible with pure argon shielding gas. With reactive shielding gases, the stream of molten filler metal droplets from the electrode is less focused and is spread out over a larger area of the

weld pool. This causes an increase in weld width. The large filler metal droplet impingement area, the less focused and more lateral flow of molten filler metal droplets and the extra opposing viscous drag force from the large fusion boundary reduce the overall momentum of the backward flow of molten weld metal in the weld pool, thereby allowing higher welding speeds without humping. Thus, use of reactive shielding gases will allow further improvements in productivity.

In addition to using gravity and shielding gas, the swinging action of the filler metal droplets during detachment reduces the vertical component of the droplets' velocity, increases the impingement area and avoids focusing all of the filler metal droplets on the inclined surface of the leading edge of the gouged weld pool. As a result, the swinging instability of spray transfer with argon shielding gas at higher welding currents helps to suppress the humping phenomenon.

Acknowledgements

This work was supported by the Natural Sciences and Engineering Research Council of Canada (NSERC), and the Ontario Research and Development Challenge Fund (ORDCF) and its partners Alcan International, Babcock & Wilcox, Canadian Liquid Air Ltd, Centerline (Windsor) Ltd, John Deere, Magna International Inc. and Ventra. Loan of robotic GMA welding equipment by Lincoln Electric Company of Canada Ltd and Fanuc Robotics Canada Ltd is gratefully acknowledged. The TIME shielding gas used in this study was supplied by BOC Gas.

References

1. B. Cary: 'Modern welding technology', 5th edn, 477; 2002, Toronto, Prentice Hall Canada Inc.
2. K. Nishiguchi, K. Matsuyama, K. Terai and K. Ikeda: in Proc. 2nd Int. Symp. JWS 'Advanced welding technology', Paper 2-2-(10); 1975, Osaka, Japan Welding Society.
3. B. J. Bradstreet: *Weld. J.*, 1968, **47**, (6), 314s–322s.
4. K. Nishiguchi and A. Matsunawa: in Proc. 2nd Int. Symp. JWS 'Advanced welding technology', Paper 2-2(5); 1975, Osaka, Japan Welding Society.
5. T. Yamamoto and W. Shimada: in Proc. 2nd Int. Symp. JWS 'Advanced welding technology', Paper 2-2-(7); 1975, Osaka, Japan Welding Society.
6. F. Savage, E. F. Nipples and K. Agusa: *Weld. J.*, 1979, **58**, (7), 212s–224s.
7. S. Hiramoto, m. Ohmine, t. Okuda and A. SHINMI: in Proc. Int. Conf. 'Laser advanced material processing – science and spplication', 157–162; 1987, Osaka, High Temperature Society of Japan and Japan Laser Processing Society.
8. C. E. Albright and S. Chiang: *J. Laser Applic.*, 1988, **1**, (1), 18–24.
9. S. Tsukamoto, H. Irie, M. Inagaki and T. Hashimoto: *Trans Nat. Res. Inst. Metals*, 1983, **25**, (2), 62–67.
10. S. Tsukamoto, H. Irie, M. Inagaki and T. Hashimoto: *Trans Nat. Res. Inst. Metals*, 1984, **26**, (2), 133–140.
11. M. Tomie, N. Abe and Y. Arata: *Trans JWRI*, 1989, **18**, (2), 175–180.
12. W. Shimada and S. Hoshinouchi: *J. JWS*, 1982, **51**, (3), 280–286.
13. P. F. Mendez, K. L. Niece and T. W. Eagar: in Proc. Int. Conf. 'Joining of advanced and specialty material II'; 1999, Cincinnati, OH, ASM International.
14. P. F. Mendez and T. W. Eagar: *Weld. J.*, 2003, **82**, (10), 296s–306s.
15. U. Gratzke, P. D. Kapadia, J. Dowden, J. Kross and G. Simon: *J. Physics D: Appl. Physics*, 1992, **25**, (11), 1640–1647.
16. E. O. Paton, S. L. Mandel'berg and B. G. Sidorenko: *Avt. Svarka*, 1971, **24**, 1–6.
17. Control Vision: 'LaserStrobe Model 4Z – operation manual'; 1999, Idaho Fall, ID, Control Vision Inc..
18. N. Rajaratnam: 'Turbulent jets', 1st edn, 211; 1976, New York, American Elsevier Publishing Company Inc.
19. M. Beck, P. Berger, F. Dausinger and H. Hügel: in Proc. 8th Int. Symp. 'Gas flow and chemical lasers', 769–774; 1990, Madrid, International Society for Optical Engineering.
20. Y. Arata and E. Nabegata: *Trans. JWRI*, 1978, **7**, (1), 101–109.
21. N. Yamauchi and T. Taka: 'Bead formation in TIG welding', IIW Doc. No. 212G-437-78; 1978.
22. N. Yamauchi and T. Taka: 'TIG arc welding with hollow tungsten electrode', IIW Doc. No. 212G-452-79; 1979.
23. M. M. Schwartz: 'ASM handbook', Vol. 6, 'Welding, brazing and soldering', (ed. T. B. Zoro and F. Reidenbach), 115; 1997, Materials Park, OH, ASM International.
24. S. Subramaniam and D. R. White: *Metall. Trans. B*, 2001, **32B**, (2), 313–318.
25. S. Schiaffino and A. A. Sonin: *J. Fluid Mech.*, 1997, **343**, 95–110.
26. M. Ushio, K. Ikeuchi, M. Tanaka and T. Seto: *Trans JWRI*, 1993, **22**, (1), 7–12.